This is a peer-reviewed manuscript that has been accepted for publication at *Earth and Planetary Sciences Letters* (accepted 28/09/21)

Boron isotope evidence for devolatilized and rehydrated recycled materials in the Icelandic mantle source

Edward W. Marshall[1*], Eemu Ranta[1], Sæmundur Ari Halldórsson[1], Alberto Caracciolo[1], Enikő Bali[1], Heejin Jeon[2], Martin J. Whitehouse[2], Jaime D. Barnes[3], Andri Stefánsson[1]

[1]: Nordic Volcanological Center, Institute of Earth Sciences, University of Iceland, Reykjavik, Iceland

[2]: Department of Geosciences, Swedish Museum of Natural History, Stockholm, Sweden

[3]: Department of Geological Sciences, The University of Texas at Austin, Austin, TX 78712, United States.

[*]: corresponding author, edmarshall@hi.is

ABSTRACT

Enriched mantle heterogeneities are widely considered to be generated through subduction, but the connections between specific subducted materials and the chemical signatures of mantle heterogeneities are not clearly defined. Boron is strongly isotopically fractionated at the surface and traces slab devolatilization, making it a potent tracer of previously subducted and recycled materials. Here, we present high-precision SIMS boron concentrations and isotope ratios on a comprehensive suite of quenched basaltic glasses from all neovolcanic zones in Iceland, two rhyolite glasses, and a set of primitive melt inclusions from central Iceland. Boron isotope ratios ($\delta^{11}B$) in Icelandic basalts and melt inclusions range from -11.6‰ to -1.0‰, averaging -4.9‰, which is higher than mid-ocean ridge basalt (MORB; $\delta^{11}B$ = -7.1‰). Because the $\delta^{11}B$ value of the Icelandic crust is low, the high $\delta^{11}B$ compositions of the Icelandic lavas are not easily explained through crustal assimilation processes.

Icelandic basalt glass and melt inclusion B/Ce and $\delta^{11}B$ values correlate with trace element ratio indicators of the degree of mantle partial melting and mantle heterogeneity (e.g. Nb/Zr, La/Yb, Sm/Yb), which indicate that the boron systematics of basalts are controlled by mantle heterogeneity. Additionally, basalts with low B/Ce have high $^{206}Pb/^{204}Pb$, further indicating mantle source control. These correlations can be used to deduce the boron systematics of the individual Icelandic mantle components. The enriched endmember within the Iceland mantle source has a high $\delta^{11}B$ value and low B/Ce, consistent with the composition of "rehydrated" recycled oceanic crust. The depleted endmember comprises multiple distinct components with variable B/Ce, likely consisting of depleted MORB mantle and/or high $^{3}He/^{4}He$ mantle and two more minor depleted components that are consistent with recycled metasomatized mantle wedge and recycled slab gabbro.

The compositions of these components place constraints on the devolatilization history of recycled oceanic crust. The high $\delta^{11}B$ value and low B/Ce composition of the enriched component within the Iceland mantle source is inconsistent with a simple devolatilization process and suggests that the recycled oceanic crust component may have been isotopically overprinted by B-rich fluids derived from the underlying hydrated slab lithospheric mantle (i.e. "rehydration"). Further, the B/Ce and $\delta^{11}B$ systematics of other OIBs can be used to constrain the devolatilization histories of recycled components on a global scale. Globally, most OIB B/Ce compositions suggest that recycled components have lost >99% of their boron, and their $\delta^{11}B$ values suggest that rehydration may be a sporadic process, and not ubiquitous.

1. INTRODUCTION

Subduction is considered to be the primary mechanism for the generation of enriched heterogeneities (i.e. heterogeneities rich in incompatible elements relative to the primitive mantle) in Earth's mantle. Enriched mantle heterogeneities are observed in the chemical variation of mid-ocean ridge basalts (MORBs) and, in particular, ocean-island basalts (OIBs). Such heterogeneities have classically been

62 detected using a combination of trace element and radiogenic isotope systematics,
63 constructing the "zoo" of mantle endmembers (White, 2015; Zindler and Hart,
64 1986). Trace elements and radiogenic isotope ratios have very high sensitivity to
65 the presence of enriched materials in a melting region, but enriched materials could
66 originate through a variety of processes other than the subduction of surficial
67 material (e.g. metasomatism; Workman et al., 2004 and references therein). As a
68 result, the subduction hypothesis of generating mantle heterogeneity cannot be
69 clearly tested using trace element and radiogenic isotope systematics. However,
70 stable isotopes provide a useful tool for detecting surficial materials in the mantle
71 because stable isotopes are fractionated significantly only at low temperature close
72 to Earth's surface and this low-T stable isotope signature can be detected in mantle-
73 derived materials. In the last decade, there has been increasing use of traditional
74 and non-traditional stable isotopes for identifying mantle heterogeneities and
75 tracing their provenance (e.g. H, O, N, Mg, Cl, Fe, Zn, Tl) (e.g. Blusztajn et al., 2018;
76 Hartley et al., 2021; Walowski et al., 2021, 2019; Wang et al., 2018).
77 A promising, but underutilized, stable isotope system for detecting mantle
78 heterogeneity is the boron isotope system. To date, the application of boron isotope
79 systematics for detecting mantle heterogeneities in the sources of OIBs has been
80 handicapped because boron is susceptible to contamination from crustal
81 assimilation (Genske et al., 2014; Marschall, 2018 and references therein). Seawater
82 has both a high boron concentration and an extreme boron isotope composition
83 (+39.5‰), and therefore hydrothermal overprinting is able to dramatically alter the
84 primary boron chemistry of oceanic crust (Yamaoka et al., 2012). Because nearly all
85 MORB and OIB erupt through seawater-altered oceanic crust, assimilation is a
86 constant concern in boron isotope studies of MORB and OIB (Marschall, 2018).
87 Previously, high-precision boron isotope analyses of low-[B] materials, such as
88 basalts, could only be performed via MC-ICP-MS or TIMS, which required time-
89 intensive chemical extraction of boron within a specialized clean laboratory facility.
90 Consequently, boron isotope studies of OIBs and MORBs have been made more
91 slowly than for other easier-to-measure light stable isotope systems (e.g., H, O).
92 However, more recently there has been refinement of a high-precision SIMS-based

boron isotope analysis technique, which permits fast *in-situ* analysis of boron isotope ratios (Marschall and Monteleone, 2015). Furthermore, ambiguity in the boron isotope composition of MORB has recently been clarified by Marschall et al. (2017). Given these new developments, boron isotopes can be employed more easily as tool to detect recycled crustal components at localities unaffected by the assimilation of seawater-altered oceanic crust.

Iceland is an ideal hotspot locality for a boron isotope study of mantle heterogeneities, as it is an OIB locality located along a subaerial section of the mid-ocean ridge and therefore is not altered by seawater. Icelandic basalts are diverse in composition: ranging from depleted picrites to alkali basalts (e.g. Jakobsson et al., 2008; Peate et al., 2010; Stracke et al., 2003; Thirlwall et al., 2004, and references therein). Decades of geochemical work on Icelandic basalts has produced a well-constrained model of the nature of heterogeneity in the Icelandic mantle source. Building on this prior characterization, stable isotope studies of the Icelandic mantle can robustly estimate the endmember compositions of recycled components within the Icelandic mantle source (Halldórsson et al., 2016a, 2016b; Magna et al., 2011). Additionally, a wide variety of Icelandic materials have been previously studied for their boron concentration and isotope ratios (Brounce et al., 2012; Gurenko and Chaussidon, 1997; Hartley et al., 2021; Raffone et al., 2010; Rose-Koga and Sigmarsson, 2008). This previous characterization provides a groundwork for a comprehensive survey and evaluation of boron isotope compositions in Icelandic basalts.

Here, we present high-precision SIMS boron isotope measurements of a geochemically diverse suite of Icelandic quenched basaltic glasses, rhyolites, and basaltic melt inclusions. In contrast to previous studies, we find that the boron isotope compositions of Icelandic basalts correlate with mantle source heterogeneity, and range in composition from depleted basalts with boron isotope ratios similar to MORB to enriched basalts with boron isotope ratios higher than MORB. We use boron isotope systematics to place constraints on the origin of the depleted and enriched components. We further show that the boron isotope

composition of enriched components in the mantle can place constraints on the devolatilization history of that component during its subduction.

2. GEOLOGICAL SETTING

Iceland is a large (>100,000 km^2) plateau divided by the mid-ocean ridge system that lies above sea level as a result of increased lithospheric thickening and plume-driven buoyant uplift by the underlying Icelandic mantle plume (Bjarnason and Schmeling, 2009). Unlike most volcanic islands, the Icelandic plateau has no known submarine periods and appears to have remained above sea level throughout its history (Denk et al., 2011; Harðarson et al., 2008). Volcanism in Iceland is confined to several volcanic zones, some of which represent the subaerial extent of the mid-ocean ridge rift axis and others represent lower-volume off-rift "flank" volcanism related to shear zones and areas of incipient propagating rift. Volcanic zones along the rift axis include (See Fig. 1): the Reykjanes Peninsula (RP), the Western Rift Zone (WRZ), Eastern Rift Zone (ERZ), and Northern Rift Zone (NRZ). Off-rift areas of volcanism include the South Iceland Volcanic Zone (SIVZ) and Snæfellsnes Volcanic Zone (SNVZ). Magmatism along the rift axis is dominantly composed of subalkaline picritic to basaltic tholeiitic lavas, whereas magmatism in off-rift zones is composed of transitional alkalic to alkalic lavas (Jakobsson et al., 2008). More evolved lavas, such as icelandite (i.e. the tholeiitic equivalent of andesite) and rhyolite, appear both along the rift axis and in off-rift areas, but are rarer than basaltic lavas in the volcanic pile.

3. SAMPLES

Four different sample types were used in this study, each representing a rock specimen from an individual locality: subglacially-quenched basalt, icelandite, and rhyolite glasses (n = 43), basaltic tephra (n = 2), and plagioclase-hosted and olivine-hosted basaltic melt inclusions (n = 15; from three different localities in the ERZ). The studied basalt samples collectively span the full variability of major and trace

element chemistry in Icelandic basaltic lavas, ranging from tholeiitic and extremely depleted basaltic glasses (MID-1), to alkaline and highly enriched basalts (OLAF-1). Additionally, obsidian rhyolitic glasses were included in this study, A-THO and A-ALK. Both rhyolites were previously studied in Óskarsson et al. (1982), Hemond et al. (1993), and Halldórsson et al. (2016a). The subglacial glasses are sampled from quenched pillow rims in subglacial volcanic edifices erupted during the Brunhes geomagnetic epoch at the end of the Pleistocene (0.78 to 0.01 Ma). This complete sample set (See Fig. 1 for their locations) permits us to determine the variability of boron isotope compositions, constrain the effects of assimilation (including the influence of seawater on basalt samples erupted in seawater dominated areas; i.e. REY-1 and SURT-1), and understand the controls on boron isotope compositions. The majority of these glasses (excluding the KVK-200-series samples) have been included in a number of prior studies targeting subglacial glasses associated with the Iceland hotspot (Barry et al., 2014; Caracciolo, 2021; Caracciolo et al., 2020; Füri et al., 2010; Halldórsson et al., 2016a, 2016b; Macpherson et al., 2005; Rasmussen et al., 2020).

Plagioclase-hosted and olivine-hosted basaltic melt inclusions and their host glasses were collected from Fontur (tephra), Saxi (tephra), and Ljósufjöll (subglacial pillow rim) in the Veiðivötn fissure swarm in the Eastern Rift Zone (Caracciolo et al., 2020). The pre-eruptive storage pressure and chemical composition of the melt inclusions and host glasses were previously characterized in Caracciolo et al. (2020). All melt inclusions are glassy and affected by minor post-entrapment processing. Melt inclusions permit testing of whether mid- and lower-crustal melts (as sampled by melt inclusions) have different compositions than erupted basalts (as sampled by quenched glasses).

4. METHODS

Boron concentration and isotope analyses were performed on a CAMECA IMS 1280 secondary ion mass spectrometer (SIMS) at the NordSIMS facility in Stockholm, Sweden. An Oregon Physics Hyperion H201 RF plasma source was used

185 to generate a high-intensity (80nA) primary beam of O^- ions. Both B isotopes were
186 collected simultaneously on two electron multipliers in multicollection mode.
187 Multicollection allows more counts to be collected in less time relative to single
188 collection and improves analysis precision, as analysis precision at such low
189 concentrations is nearly entirely controlled by Poisson counting statistics (Fig. S1).
190 Using this method, a typical single-spot analysis (~25 min) has a precision of
191 ~1.5‰ (2SD) for a sample with 1 µg/g B, an improvement in single-spot precision
192 over recent SIMS boron isotope studies (e.g. 2‰ to 4‰ (2SD) at 1 µg/g B;
193 Marschall and Monteleone, 2014; Walowski et al., 2019; Hartley et al., 2020).
194 Reference materials StHs6/80-G and GOR132-G were used as a calibrating standard
195 and as a secondary standard, respectively, for the isotope measurements (Jochum et
196 al., 2006). The reproducibility of StHs6/80-G varied between 0.43‰ and 1.84‰
197 (2SD). The measured composition of GOR132-G agreed with the published
198 composition of the reference material within uncertainty. No matrix effect was
199 detected between the andesitic StHs6/80-G and komatiitic GOR132-G reference
200 materials. Some samples in this study have been analyzed for $\delta^{11}B$ in previous
201 studies and we reproduce their results within uncertainty (MID-1, A-THO, A-ALK;
202 Gurenko and Chaussidon, 1997; Rose-Koga and Sigmarsson, 2008).
203 Major element analyses were performed via electron microprobe analysis at
204 the University of Iceland on a JEOL JXA-8230 Superprobe. Trace element analysis of
205 most subglacial glasses were performed via solution inductively coupled plasma
206 mass spectrometry (ICP-MS) at the Scripps Institution of Oceanography on a
207 Thermo-Fisher Element 2 mass spectrometer. Trace element analyses of the KVK-
208 200-series samples were performed via laser ablation single collector ICP-MS at the
209 Geological Society of Finland on a Nu AttoM mass spectrometer. Oxygen isotope
210 ratios in glasses were measured via laser fluorination at the University of Texas at
211 Austin on a ThermoElectron MAT 253. Details on the analytical methods can be
212 found in the supplementary methods.
213
214 **5. RESULTS**
215

5.1 Boron concentrations

Boron concentrations in the subglacial basalts and icelandites (n = 44, SiO_2 = 45.7 to 56.9 wt%) range from 0.17 to 5.69 µg/g (Fig. 2). Boron concentrations in the two rhyolite samples (SiO_2 = 72.9 and 74.5 wt%) are 5.42 and 15.2 µg/g B. Basaltic melt inclusions and basalts have very similar boron concentrations at a given MgO. In the basalts (both glasses and melt inclusions), boron concentration, as well as the concentration of other incompatible elements, is strongly negatively correlated with MgO (Fig. 2a). The most primitive basalt samples (~9.75 wt% MgO) have the lowest B concentration (0.17 µg/g), whereas the lowest MgO basalts (~4.0 wt% MgO) have the highest B concentration among Icelandic basalts (3.37 µg/g). Samples from SNVZ fall off the main MgO-B trend to lower B concentrations at a given MgO and samples from the SIVZ fall off the trend to higher B concentrations. At a given MgO, Icelandic basalts tend to have lower B concentrations than MORBs (Fig. 2a). Samples measured in this study have comparable B concentrations at a given MgO to samples in previous Icelandic studies, although there is a tendency for Icelandic basalts and melt inclusions to anomalously fall to low [B] at a given MgO (e.g Brounce et al., 2012; Gurenko and Chaussidon, 1997; Hartley et al., 2020).

Boron shows strong covariation with minor (Fig. 2b) and incompatible lithophile trace elements (Fig. S3). Only enriched samples from SNVZ fall off the correlations toward lower B content. Consistent with observations at other OIB localities (Chaussidon and Marty, 1995; Genske et al., 2014; Ryan et al., 1996; Walowski et al., 2019), average B/Ce for Icelandic subglacial basalts and basaltic melt inclusions is 0.052 ±0.027, lower than the typical MORB value of 0.09 (Marschall et al., 2017) (Fig. 2c). The B/Ce of Icelandic basalts negatively correlates with indicators of degree of partial melting and source heterogeneity (e.g. La/Yb) such that low La/Yb basalts have approximately MORB-like compositions and high La/Yb basalts have low B/Ce compositions.

5.2 Boron isotope compositions

Measured boron isotope compositions from the subglacial basalt glass suite ranges from -9.2‰ to -1‰ with a mean of -4.3‰ (Fig. 3). The majority of glasses

fall within a range of -6.4‰ to -1.9‰ (90% of measured samples). The two rhyolite samples both have $\delta^{11}B$ values greater than 0‰, higher than all other samples in this study (Fig 3). Individual basaltic melt inclusions show wide variability (-11.6‰ to -3.7), but the average melt inclusion at each locality has a nearly identical average $\delta^{11}B$ value as its host glass (Table 1), similar to the observations of previous studies (e.g. Hartley et al., 2020).

The basalt glass and melt inclusion $\delta^{11}B$ values have a weak negative correlation with MgO ($R^2 = 0.17$), and variability in $\delta^{11}B$ decreases with decreasing MgO, so that basalt samples with MgO > 8 wt% have $\delta^{11}B$ values ranging from -9.2‰ to -2.3‰ but samples with MgO < 5 wt% range from -4.1‰ to -1.7‰ (Fig. 4a). Similarly, basalt glass and melt inclusion $\delta^{11}B$ values are weakly positively correlated with B concentration (Fig. 5), and with indicators of degree of partial melting and source heterogeneity (e.g. Nb/Y, La/Yb) (Fig. 4b, Fig. S4). Icelandic basalt and melt inclusion $\delta^{11}B$ values are higher than those for MORB, averaging -4.9‰ and -7.1‰ respectively (Marschall et al., 2017).

6. DISCUSSION

6.1 Do high $\delta^{11}B$ signatures in Icelandic basalts originate from the crust or mantle?

If Icelandic basalts sampled only depleted MORB mantle (DMM) and/or primitive mantle, then their boron isotope compositions should have a distribution similar to uncontaminated MORB, that is, having a weighted mean of -7.1‰ and a standard deviation of 2.8‰ (2SD) (Marschall et al., 2017). However, Icelandic basalts measured in this study (i.e. samples with MgO > 4 wt.%) instead have a mean of -4.9‰ and standard deviation of 4.2‰ (2SD) (Figs. 3 and 4). A t-test comparing the $\delta^{11}B$ values of MORB and our suite of Icelandic basalts shows that the difference in mean $\delta^{11}B$ value between the two groups is highly statistically significant ($p < 0.0001$, $n = 45$). This difference continues to be statistically significant ($p = 0.0033$, $n = 12$) when the dataset is conservatively filtered to include

only the most primitive and pristine basalt samples, and exclude basalts with MgO < 8 wt%, Cl/K > 0.08, or $\delta^{18}O$ < +4.5‰. This compositional difference strongly suggests that a component besides DMM contributes boron to the basalts and generates a difference in mean $\delta^{11}B$ value from MORB. However, it is not clear whether this shift in the basalt boron isotopic composition is derived from the mantle source or is a result of crustal assimilation. In the following sections, we will systematically evaluate secondary (crustal) processes which may act to modify primary (mantle-derived) $\delta^{11}B$ characteristics of Icelandic basalts.

6.1.1 Assimilation of seawater-derived components in the Icelandic crust

One way to explain why Icelandic basalts have on average higher $\delta^{11}B$ values than MORBs is through the assimilation of high $\delta^{11}B$ value seawater-altered basaltic crust. In oceanic settings, Cl/K ratios are typically used to evaluate the degree of assimilation because seawater altered oceanic crust has high [Cl]. However, Iceland represents a subaerial portion and meteoric water dominated section of the Mid-Atlantic Ridge. Consequently, alteration by seawater-derived fluids does not occur substantially within the Icelandic crust. However, some samples were erupted near the coast or even at sea (i.e. REY-1 and SURT-1) and could have been affected by seawater contamination. Regardless, both REY-1 and SURT-1 have Cl/K ratios below 0.08, indicating a lack of contamination by high Cl/K seawater-derived components (Michael and Cornell, 1998), and have $\delta^{11}B$ values similar to basalts sampled farther inland, demonstrating no relationship between proximity to the sea and anomalous boron isotope composition. (For further discussion of a high $\delta^{11}B$ altered component in the Icelandic crust see the Supplementary Information)

6.1.2 Assimilation of rhyolite-components in the Iceland crust

Assimilation of high $\delta^{11}B$ (-2‰ to +16.9‰) rhyolite into Icelandic basalt could, in theory, explain why Icelandic basalts have higher $\delta^{11}B$ compositions than MORB (Rose-Koga and Sigmarsson, 2008). Basalt-rhyolite binary mixing

calculations (Fig. S5) suggest that only 4% assimilation of a typical rift rhyolite (~5 μg/g B, $\delta^{11}B$ = ~+5‰) into a primitive Icelandic basalt with a MORB-like boron isotope composition (0.5 μg/g B, $\delta^{11}B$ = -7.1‰) is needed to produce the high $\delta^{11}B$ compositions observed in Icelandic basalts (i.e. ~-3‰).

However, rhyolite is a spatially restricted and relatively uncommon lithology in the Icelandic crust and is therefore not consistent with ubiquitously observed high $\delta^{11}B$ basalts. Furthermore, although rhyolite assimilation could successfully explain high $\delta^{11}B$ values, such assimilation would have a large impact on the trace element composition of Icelandic basalts. Depleted basalts with high $\delta^{11}B$ values like NAL688 and A9 are very difficult to explain through rhyolite assimilation. The quantity of rhyolite needed to increase their $\delta^{11}B$ values to their current compositions of -2.9‰ and -5.1‰, respectively, would also enrich the basalts in incompatible trace elements, which is not observed (Fig. S5).

6.1.3 Bulk assimilation of the altered Icelandic upper crust

A fundamental problem with explaining high $\delta^{11}B$ values in Icelandic basalts through the assimilation of bulk altered Icelandic upper crust is that the altered Icelandic upper crust is expected to have a low $\delta^{11}B$ value. Alteration of rock by meteoric water will result in a decrease in the $\delta^{11}B$ value of the rock, as meteoric water has a negligible B content relative to the rock and because $\Delta^{11}B_{fluid\text{-}mineral}$ is positive for all common alteration minerals (e.g. clays, carbonates; Hervig et al. 2002, and references therein). Therefore, as meteoric water alteration progresses, the crust will be forced to low $\delta^{11}B$ compositions. For example, secondary minerals in Icelandic meteoric water-dominated hydrothermal systems have $\delta^{11}B$ values significantly lower than most basalts or hydrothermal fluids (i.e. -22‰, Aggarwal et al., 2000). Additionally, altered Biscuit Basin rhyolite in Yellowstone (a meteoric water-dominated locality) has lower $\delta^{11}B$ values than unaltered Biscuit Basin rhyolite (Palmer and Sturchio, 1990). Therefore, assimilated crust is expected to have a lower $\delta^{11}B$ value than primitive basalt, and the addition of bulk altered Icelandic upper crust into primitive melts should decrease their $\delta^{11}B$ value (Brounce

et al., 2012). For further discussion on the boron systematics of hydrothermal fluids and altered rocks in Iceland, see the Supplementary Information.

Although $\delta^{18}O$ values record assimilation processes in Icelandic basalts, assimilation will not affect $\delta^{18}O$ and $\delta^{11}B$ to the same degree. Low $\delta^{18}O$ values in Icelandic basalts are commonly invoked as evidence that Icelandic basalts have assimilated low-$\delta^{18}O$ hydrothermally altered material in the crust (e.g. Bindeman et al., 2008). In the case of oxygen, the $\boxed{[O]_{assimilant}/[O]_{melt}}$ is always approximately one, whereas for boron, $\boxed{[B]_{assimilant}/[B]_{melt}}$ has a wide range of potential values (from ~0.05 to ~60). Therefore, assimilation should not always result in consistent behavior of the $\delta^{18}O$ and $\delta^{11}B$ systems, and it is expected that the two systems will be decoupled when materials with very high or low $\boxed{[B]_{assimilant}/[B]_{melt}}$ are assimilated. Additionally, the mantle source of Iceland may have a low $\delta^{18}O$ component, and therefore melts with $\delta^{18}O$ as low as +4.5‰ may not have assimilated any crust (Maclennan et al., 2003; Thirlwall et al., 2006). Figure 5 presents mixing and AFC model calculations between primitive melts and the estimated compositions of two potential crustal components: bulk meteoric water-altered Icelandic upper crust (orange lines) and crust that has been extensively altered in a high-T meteoric water recharged hydrothermal system (blue lines) (see Supplementary Information for details on these components). The AFC curves in Figure 5a move quickly towards low $\delta^{11}B$ as $\delta^{18}O$ decreases, and are unable to explain the relatively MORB-like $\delta^{11}B$ values (~-7‰) of melts at very low $\delta^{18}O$ values (<+3.5‰). The failure of geochemical models to clearly explain the assimilation process in $\delta^{11}B$- $\delta^{18}O$ space suggests that a method that only uses $\delta^{18}O$ values to assess the influence of assimilation on $\delta^{11}B$ systematics will likely be inaccurate.

Rather, using the relationships between [B] and $\delta^{11}B$ values is likely more robust than using $\delta^{18}O$ for assessing the effect of crustal assimilation on the $\delta^{11}B$ values of basalts. Figure 5b shows that the distribution of Iceland basalt and melt inclusion $\delta^{11}B$ values can be explained by mixing and AFC models of crustal components into otherwise uncontaminated fractionating melts. Mixing and AFC

processes push melt compositions toward higher [B] and lower $\delta^{11}B$ values (solid and dashed curves, Figure 5b). Because many previously measured Icelandic basalts lie within the high [B] and low $\delta^{11}B$ value region that is defined by the model curves, this suggests that many previously measured Icelandic basalts have experienced assimilation that affected their $\delta^{11}B$ values. For example, basalts from Lakigígar lie at the end of these AFC and mixing curves and imply that Lakigígar basalts have assimilated large amounts of crust (these models suggest addition of ca. 30-40% of high-T meteoric water altered crust with variable $\delta^{11}B$ values). High degrees of assimilation are consistent with the results of Brounce et al. (2012) and Bindeman et al. (2008), who estimated assimilation rates of 30 to 35%. In contrast, the basalts measured in this study lie at the start of these mixing and AFC curves and suggest that the melts sampled in this study have been minimally contaminated by crust. Moreover, the samples presented in this study have high $\delta^{11}B$ values at a given boron content relative to previously measured Icelandic basalt samples, which suggests that the samples in this study have been less affected by crustal assimilation than previously studied Icelandic basalt samples. Therefore, the basalts measured in this study are unlikely to have been significantly overprinted by secondary assimilation processes.

Finally, melt inclusions can also place constraints on the effect of assimilation. Melt inclusions represent melts trapped at depth within crystals and are therefore potentially less crustally contaminated than their matrix glasses. In fact, there is no relationship between melt inclusion $\delta^{11}B$ and melt inclusion equilibration depth that suggests the influence of assimilation in the upper crust (Fig. S6). Additionally, the average $\delta^{11}B$ value of melt inclusions from each sample is usually indistinguishable (within uncertainty) from the composition of the sample matrix glass (see Table 2). This similarity suggests that as a population, melt inclusions are not less crustally contaminated than their matrix glasses. However, it is important to note that some Icelandic melt inclusions have very low $\delta^{11}B$ compositions (as low as -20.7‰; Hartley et al. 2020), which may indicate that boron can be locally strongly affected by assimilation processes. Regardless, we conclude that the observed high $\delta^{11}B$ values of basalt glasses and melt inclusions is

not consistent with crustal contamination processes and may rather be mantle derived.

6.2 Mantle source control of boron in Icelandic basalts

The high boron isotope compositions of Icelandic basaltic magmas may reflect a mantle source signature, particularly given that assimilation cannot explain their high $\delta^{11}B$ values. If so, then the boron isotope compositions of Icelandic basalts (i.e. samples with MgO > 4 wt%) are expected to correlate with indices of mantle source processes and variability. In fact, a key feature of our data is a consistent correlation between Icelandic basalt $\delta^{11}B$ values and trace element indices of degree of partial melting and source heterogeneity: Nb/Y (Fig. 4b), La/Sm, Sm/Yb, La/Yb, Nb/Zr, K_2O, Zr/Sm, B/Yb, and Zr/Y (see Fig. S4). Although the observed correlations have low R^2 values (less than 0.28) they are highly statistically significant (*p* values < 0.0027, or better than 3σ confidence), and such correlations consistently appear between $\delta^{11}B$ values and trace element ratio indices of mantle heterogeneity. The correlations remain statistically significant even when all samples with $\delta^{18}O$ values less than +4.5‰ (i.e. those likely to have experienced assimilation) are removed. The low R^2 values of the correlations are a natural result of the relatively large uncertainty of the $\delta^{11}B$ analysis, scatter due to stochastic melt aggregation processes (see Rudge et al. 2013), and isotopic variability within the mantle endmember components. Therefore, we conclude that there is a robust correlation in Icelandic basalts between basalt $\delta^{11}B$ values and trace element ratio indices of partial melting and mantle source heterogeneity.

Previous studies of Icelandic basalts have identified similar correlations between the same trace element ratios and $^{143}Nd/^{144}Nd$ or $^{87}Sr/^{86}Sr$, indicating that these trace element ratios are reliable indicators of mantle heterogeneity in Icelandic basalts (Fig. S7) (e.g. Kokfelt et al., 2006; Shorttle and Maclennan, 2011). Such correlations in Icelandic basalts are the product of progressive melting of a heterogeneous mantle in which fusible and enriched heterogeneities are

preferentially sampled by melts at low degrees of partial melting, and refractory and depleted heterogeneities are preferentially sampled at higher degrees of partial melting (Shorttle and Maclennan, 2011). Because basalts with enriched compositions have higher $\delta^{11}B$ values, this suggests that enriched heterogeneities in the Icelandic mantle source have high $\delta^{11}B$ values. Similarly, because depleted basalts have lower $\delta^{11}B$ values, this suggests that depleted heterogeneities in the Icelandic mantle source have lower $\delta^{11}B$ values (Fig. 6b).

Like $\delta^{11}B$ values, B/Ce ratios appear to be controlled by mantle heterogeneity and correlate with trace element indices of mantle heterogeneity, further highlighting the mantle source control of boron in Icelandic basalts (Fig. 6a, see also Fig. S8). B and Ce have nearly identical incompatibilities, and therefore the B/Ce ratio can be used as an indicator of the degree of source enrichment of B relative to Ce (Marschall et al., 2017). Although Figure 6a shows that B/Ce is high in depleted basalts but low in enriched basalts, the actual B concentration of the enriched component is still higher than the B content of the depleted component because the enriched source has much higher Ce content. For example, assuming B/Ce is not significantly fractionated during melting, the approximate B content of the depleted and enriched components can be calculated from the observed B/Ce of the enriched and depleted basalts (~0.025 and ~0.1, respectively) and the proposed Ce content of the enriched and depleted Icelandic mantle components (8.161 μg/g and 0.55 μg/g Ce, respectively; Koornneef et al., 2012). This calculation results in 0.20 μg/g B for the enriched component and 0.055 μg/g B for the depleted component. Therefore, the depleted component has a boron concentration that is roughly similar to the B content of DMM (0.077 μg/g B; Marschall et al., 2017), and the enriched component has a boron content that is noticeably higher than the depleted component.

6.3 Boron characteristics of enriched and depleted heterogeneities in the Icelandic mantle source

6.3.1 *Boron characteristics of the depleted component*

Depleted basalts measured in this study can place constraints on the B/Ce and $\delta^{11}B$ value of depleted components within the Icelandic mantle source (Fig. 6). By focusing on the most depleted quartile of Icelandic basalts (which have similar La/Yb to MORBs), one can more precisely compare the B characteristics of depleted Icelandic basalts to MORBs to test for the influence of recycled or plume components. The lowest La/Yb quartile of Icelandic basalts overlaps with the boron chemistries of MORB, but with key differences. First, low La/Yb basalts do not have equivalent $\delta^{11}B$ values to MORB, but instead fall to higher values reflecting differences in source composition ($p < 0.05$; see Fig. S9). Second, melt inclusions make up a portion of the low La/Yb population and these melt inclusions have much lower B/Ce than MORB. Lastly, low La/Yb basaltic glasses have MORB-like to higher than MORB B/Ce that suggests a distinct third component from the low B/Ce melt inclusions and more MORB-like B/Ce samples. These different observations can be explained, with some speculation, by the presence of distinct mantle geochemical components within the Icelandic mantle source. The basalts with MORB-like B/Ce and $\delta^{11}B$ values likely reflect a mixture of DMM and, as primitive mantle should have very similar B/Ce and $\delta^{11}B$ value as DMM, depleted ancient high $^{3}He/^{4}He$ plume component (see Jackson et al., 2020). The high B/Ce basaltic glasses indicate the melting of a high B/Ce source, such as mantle wedge material that has been enriched in boron and isotopically overprinted by a high B/Ce agent to high $\delta^{11}B$ values by slab-derived fluid or arc melts (Walowski et al., 2021). Finally, the low B/Ce, depleted compositions, and MORB-like $\delta^{11}B$ values of the melt inclusions may reflect the composition of recycled depleted, and devolatilized slab gabbros (Stracke et al., 2003a). This model is consistent with previous recycled gabbro-invoking models for explaining the observed positive Ba and Sr anomalies in depleted Icelandic melts (Kokfelt et al., 2006).

6.3.2 *Boron characteristics of the enriched component*

The compositions of enriched Icelandic basalts can place constraints on the composition of the enriched component in the Icelandic mantle source (Fig. 6). The boron systematics of enriched, high La/Yb basalts is simpler than for the depleted basalts: as La/Yb increases the $\delta^{11}B$ value of Icelandic basalts increase and B/Ce decreases. In light of the demonstration by Peate et al. (2010) and Kokfelt et al (2006) that multiple enriched components exist in the Icelandic mantle source, the simplest explanation for this apparent single enriched endmember is that all enriched components sampled in this study have similar low B/Ce and high $\delta^{11}B$ characteristics. Because the most enriched basalts have $\delta^{11}B$ values as high as -1‰, the enriched component(s) within the Icelandic mantle source must have low B/Ce and a $\delta^{11}B$ value ≥ -1‰. This composition and the origin of the enriched component can be explained as devolatilized oceanic crust that has undergone overprinting by fluids from the serpentinized lithospheric mantle from the slab, a process called 'rehydration' (see section 6.4).

Despite that only a subset of our samples (n=16) has been measured for $^{206}Pb/^{204}Pb$, samples with radiogenic $^{206}Pb/^{204}Pb$ have low B/Ce (0.05 to 0.005) and samples with unradiogenic $^{206}Pb/^{204}Pb$ have higher, MORB-like B/Ce (0.14 to 0.05; Fig. 7). Although unradiogenic and radiogenic $^{206}Pb/^{204}Pb$ isotope compositions do not neatly correspond to depleted and enriched Icelandic mantle components as defined by trace elements, radiogenic $^{206}Pb/^{204}Pb$ ratios are indicative of large time-integrated U/Pb that is consistent with recycled subducted oceanic crust that has undergone Pb-loss (e.g. Thirlwall et al., 2004). Therefore, the correspondence of low B/Ce and radiogenic $^{206}Pb/^{204}Pb$ is consistent with the composition of recycled oceanic crust.

Previous studies (e.g. Peate et al., 2010) have found that enriched basalts from the SIVZ have Pb, Nd and He isotope compositions that are typical of the composition of the 'PREMA' mantle zoo endmember (PREMA = PREvalent MAntle; White, 2015). If the high $\delta^{11}B$ value, low B/Ce SIVZ basalts are representative of the PREMA component, this suggests that PREMA has high $\delta^{11}B$ value and low B/Ce (i.e. relative to DMM). This composition partially agrees with the model of Dixon et al.

(2017), which predicts PREMA to have higher $\delta^{11}B$ values than DMM, but also predicts high B/Ce. This composition also partially agrees with the findings of Walowski et al. (2019) at the PREMA-type hotspot La Réunion, who observed slightly sub-MORB B/Ce, but who also found MORB-like $\delta^{11}B$ values. Recently, Jackson et al. (2020) proposed that some SIVZ and ERZ basalts sample a primordial mantle reservoir on the basis of their high $^{3}He/^{4}He$ and anomalous ^{182}W compositions. If we filter SIVZ and ERZ samples based on the criteria of Jackson et al. (eliminate all samples with $^{3}He/^{4}He < 21R_a$), we find that the remaining samples (n = 4) have an average $\delta^{11}B$ value of -5.9 ±1.2‰. Unfortunately, equivalence testing of this average against average MORB (-7.1‰) does not clearly confirm or reject whether high $^{3}He/^{4}He$ SIVZ and ERZ lavas have $\delta^{11}B$ values distinguishable from DMM. However, this value is clearly distinct from the estimated $\delta^{11}B$ value of primitive mantle made by Gurenko and Chaussidon (1997) of ~-10‰.

6.4 Constraints on the devolatilization history of the subducted component

Enriched components in the mantle sources of Iceland and other OIB localities are often considered to be materials carried into the mantle by subducted slabs (Kokfelt et al., 2006; Halldórsson et al., 2016b; Halldórsson et al., 2016a). Subducting slabs lose fluid mobile elements as they devolatilize during their descent into the mantle, resulting in low B/Ce and Pb/Ce ratios in devolatilized slabs (Kogiso et al., 1997; Marschall et al., 2007) (Fig. 8). Consequently, the low B/Ce and Pb/Ce ratios that characterize most OIBs are thought to reflect included recycled subducted materials in the OIB source (Ryan et al., 1996). Geochemical models of the behavior of boron during slab dehydration predict that boron loss from the slab will result in very low slab $\delta^{11}B$ values (e.g. -36‰, Marschall et al., 2007; Konrad-Schmolke and Halama, 2014; Fig. 8). Melting of such ^{11}B-depleted material would be unable to reproduce the high $\delta^{11}B$ value basalt compositions observed in Iceland.

One possibility is that the slab crust has only partially devolatilized and could generate melts with higher $\delta^{11}B$ values, but such models result in high slab B/Ce, not found in Icelandic basalts. Marschall et al. (2007) found that if phengite is present

552 during devolatilization, then the B content of the slab is not dramatically reduced
553 and $\delta^{11}B$ values are not significantly fractionated to highly negative values (only
554 reaching ~-8‰). However, Marschall et al. (2007) modelled that a partially
555 devolatilized slab would contain 10 µg/g B, and if the slab has a Ce content similar to
556 the recycled component in Koornneef et al. (2012) then the partially devolatilized
557 slab would have a B/Ce of 3.18, which is not consistent with the low B/Ce of
558 Icelandic basalts (< 0.15). Further, OIBs globally have low B/Ce ratios, which
559 indicates that high B/Ce partially devolatilized materials are rare in the mantle
560 (Ryan et al., 1996).
561 Rather, the low B/Ce ratios and high $\delta^{11}B$ values of Icelandic basalts can be
562 explained by melting of devolatilized slab crust that has been metasomatically
563 overprinted by a slab rehydration process (Dixon et al., 2017; Wada et al., 2012)
564 (Fig. 8). Slab rehydration is a process that occurs in slabs that contain serpentinized
565 lithospheric mantles. As a subducting slab heats up, the hydrated lithospheric
566 mantle will dehydrate after the crust, releasing fluids that travel through the
567 overlying devolatilized crust. Devolatilized slab crust contains low volatile
568 concentrations and can be easily isotopically overprinted by high-[B] lithospheric
569 serpentinite-derived fluids (Dixon et al., 2017; Konrad-Schmolke, 2016; Konrad-
570 Schmolke and Halama, 2014; Wada et al., 2012; Walowski et al., 2015). To further
571 illustrate, thermodynamic-geochemical modelling of boron in subduction zones by
572 Konrad-Schmolke (2014, 2016) found that fluids derived from the slab lithospheric
573 mantle had high [B] and $\delta^{11}B$ values (e.g. ~40µg/g B, ~+10‰) and passed through
574 the slab crust as they ascended towards the mantle wedge. Interaction between this
575 fluid and the devolatilized slab crust increased the $\delta^{11}B$ value of the slab crust
576 without substantially increasing the slab crust B content (Fig. 8)(Konrad-Schmolke,
577 2016; Konrad-Schmolke and Halama, 2014). This process could therefore result in
578 devolatilized, low B/Ce slab crust within the deep mantle that has higher $\delta^{11}B$ values
579 than MORB. This rehydration process has also been used to explain δD values in
580 recycled slabs that are higher than MORB (Dixon et al., 2017). We therefore suggest
581 that the enriched component of the Icelandic mantle source as recycled slab crust

582 whose $\delta^{11}B$ value was overprinted by ^{11}B-rich fluids originating from its hydrated
583 lithospheric mantle.
584 OIB localities appear to have distinct B/Ce and $\delta^{11}B$ compositions that render
585 them distinct from one another and from MORB. As DMM and primitive mantle
586 domains have very similar B/Ce and $\delta^{11}B$ values, such differences are caused by
587 included subduction-derived recycled materials within the OIB mantle source that
588 have low B/Ce and high or low $\delta^{11}B$ (Fig. 8). As illustrated in Figure 8, nearly all
589 OIBs have consistently low B/Ce relative to MORB with variable $\delta^{11}B$ values,
590 suggesting that different B-depleted recycled slab materials are included in OIB
591 sources. The variation in $\delta^{11}B$ between OIB localities can be explained through the
592 sampling of distinct recycled slab crust materials that have experienced different
593 devolatilization histories or different mixtures of recycled materials. Mixing of melts
594 derived from these different mantle reservoirs is modelled in Figure 8. The four
595 dashed curves represent mixing models between MORB (yellow star) and 6%
596 partial melts of devolatilized and rehydrated slab crusts. Prior to devolatilization,
597 the slab crust boron isotope and elemental composition is +0.8‰, 26 μg/g B, and
598 8.161 μg/g Ce, respectively (Koornneef et al., 2012; Smith et al., 1995).
599 Devolatilization of the slab is modelled using a Rayleigh fractionation model with
600 different $\Delta^{11}B_{fluid\text{-}solid}$ values (three blue dashed lines in Fig. 8). Ce content is
601 assumed to not be affected by devolatilization and is fixed at the Ce content of
602 recycled pyroxenite as estimated by Koornneef et al. (2012). Rehydration is
603 assumed to increase the slab $\delta^{11}B$ value without changing B or Ce concentration, as
604 modelled in Konrad-Schmolke and Halama (2014). The mixing curves in Figure 8
605 show that Iceland's high $\delta^{11}B$ value enriched basalts are best fit by the presence of a
606 recycled slab that has been rehydrated. Hawaiian basalts fall within the cluster of
607 Icelandic basalt B/Ce-$\delta^{11}B$ compositions, suggesting that the Hawaiian and Iceland
608 hotspots have recycled components with similar devolatilization histories, that is,
609 slab devolatilization followed by rehydration. The low $\delta^{11}B$ values of Canary Islands
610 melts are best fit by a slab that has undergone simple devolatilization and Rayleigh
611 fractionation without rehydration (consistent with the conclusions of Walowski et

al., 2019). Réunion has MORB-like $\delta^{11}B$ values and is not as clearly interpretable, as it could represent either the presence of recycled materials with very low B/Ce and/or materials with MORB-like $\delta^{11}B$ values. Based on the above starting composition of the slab, the ubiquitously low B/Ce of OIBs requires that more than 99% of B is devolatilized from the slab crusts during subduction, and that less extreme devolatilization of B is not observed. In this way, the B/Ce and $\delta^{11}B$ values of OIBs can place constraints on the devolatilization history of the recycled components within the mantle sources of hotspots.

7. CONCLUSIONS

The high $\delta^{11}B$ value and low B/Ce of Icelandic basaltic melts (i.e. relative to MORB) show that the Icelandic mantle source contains recycled materials that bear the geochemical fingerprints of deep subduction processes. We find that enriched components within the Icelandic mantle source have consistently high $\delta^{11}B$ values and low B/Ce ratios, indicative of devolatilized and subsequently rehydrated recycled oceanic crust (Fig. 8). We also identify multiple depleted components that have $\delta^{11}B$ values similar to, or higher than, MORB but have variable B/Ce ratios, which are interpreted to reflect a mixture of depleted slab gabbros, slab-metasomatized residual mantle wedge, DMM, and depleted high $^{3}He/^{4}He$ plume components.

The boron isotope composition of these subducted and recycled components can be used to constrain their devolatilization history. Devolatilization of the downgoing slab will result in a boron depleted slab with low B/Ce and very low $\delta^{11}B$ values. However, the recycled materials within the Icelandic mantle source have high $\delta^{11}B$ values, which suggests that the slab crust has been overprinted by lithosphere derived fluids following crust dehydration (i.e. rehydration). Therefore, boron isotopes can place constraints on the devolatilization history of mantle heterogeneities observed at hot spots, and on the cycling of mantle volatiles through the convecting mantle.

642 Globally, nearly all OIBs have B/Ce that is less than or similar to MORB, but
643 have $\delta^{11}B$ values that may be higher, lower, or similar to MORB. Given the OIB
644 localities for which boron isotope data are currently available, this indicates that the
645 subducting slab typically undergoes extensive devolatilization and that slab
646 rehydration appears to be sporadic but not uncommon.
647
648 **Acknowledgments**
649 EWM and SAH acknowledge support from the Icelandic Research Fund (Grant
650 #195638-051 and #196139-051, respectively). Additionally, SAH and ER
651 acknowledges support from the University of Iceland Research Fund. The NordSIMS
652 facility operates under Swedish Reseach Council infrastructure grant # 2017-00671,
653 with additional support from the Swedish Museum of Natural History and the
654 University of Iceland. This is NordSIMS publication # xxx. Thomas Zack is thanked
655 for providing a generous piece of Herasil 102 glass. Brigitte Stoll and Klaus Peter
656 Jochum are thanked for kindly supplying the MPI standards. Hugh O'Brien's
657 assistance with LA-ICP-MS analyses of KVK samples is gratefully acknowledged. We
658 thank Horst Marschall and an anonymous reviewer for helpful reviews, and Rajdeep
659 Dasgupta for editorial handling.
660
661 **REFERENCES**
662 Aggarwal, J.K., Palmer, M.R., Bullen, T.D., Arnórsson, S., Ragnarsdóttir, K. V., 2000.
663 The boron isotope systematics of Icelandic geothermal waters: 1. Meteoric
664 water charged systems. Geochim. Cosmochim. Acta 64, 579–585.
665 https://doi.org/10.1016/S0016-7037(99)00300-2
666 Barry, P.H., Hilton, D.R., Füri, E., Halldórsson, S.A., Grönvold, K., 2014. Carbon isotope
667 and abundance systematics of Icelandic geothermal gases, fluids and subglacial
668 basalts with implications for mantle plume-related CO2 fluxes. Geochim.
669 Cosmochim. Acta 134, 74–99. https://doi.org/10.1016/j.gca.2014.02.038
670 Bindeman, I., Gurenko, A., Sigmarsson, O., Chaussidon, M., 2008. Oxygen isotope
671 heterogeneity and disequilibria of olivine crystals in large volume Holocene
672 basalts from Iceland: Evidence for magmatic digestion and erosion of

673 Pleistocene hyaloclastites. Geochim. Cosmochim. Acta 72, 4397–4420.
674 https://doi.org/10.1016/j.gca.2008.06.010
675 Bjarnason, I.T., Schmeling, H., 2009. The lithosphere and asthenosphere of the
676 Iceland hotspot from surface waves. Geophys. J. Int. 178, 394–418.
677 https://doi.org/10.1111/j.1365-246X.2009.04155.x
678 Blusztajn, J., Nielsen, S.G., Marschall, H.R., Shu, Y., Ostrander, C.M., Hanyu, T., 2018.
679 Thallium isotope systematics in volcanic rocks from St. Helena – Constraints on
680 the origin of the HIMU reservoir. Chem. Geol. 476, 292–301.
681 https://doi.org/10.1016/j.chemgeo.2017.11.025
682 Brounce, M., Feineman, M., LaFemina, P., Gurenko, A., 2012. Insights into crustal
683 assimilation by Icelandic basalts from boron isotopes in melt inclusions from
684 the 1783-1784 Lakagígar eruption. Geochim. Cosmochim. Acta 94, 164–180.
685 https://doi.org/10.1016/j.gca.2012.07.002
686 Caracciolo, A., 2021. Temporal evolution of crystal mush reservoirs beneath the
687 Bárðarbunga- Veiðivötn volcanic system, Iceland. University of Iceland.
688 Caracciolo, A., Bali, E., Guðfinnsson, G.H., Kahl, M., Halldórsson, S.A., Hartley, M.E.,
689 Gunnarsson, H., 2020. Temporal evolution of magma and crystal mush storage
690 conditions in the Bárðarbunga-Veiðivötn volcanic system, Iceland. Lithos 352–
691 353, 105234. https://doi.org/10.1016/j.lithos.2019.105234
692 Chaussidon, M., Marty, B., 1995. Primitive Boron Isotope Composition of the Mantle.
693 Science (80-.). 269, 383–386. https://doi.org/10.1126/science.269.5222.383
694 De Hoog, J.C.M., Savov, I.P., 2018. Boron Isotopes as a Tracer of Subduction Zone
695 Processes, in: Boron Isotopes, Advances in Isotope Geochemistry. pp. 217–247.
696 https://doi.org/10.1007/978-3-319-64666-4_9
697 Denk, T., Grimsson, F., Zetter, R., Símonarson, L.A., 2011. Late Cenozoic Floras of
698 Iceland, Topics in Geobiology. Springer Netherlands.
699 https://doi.org/10.1007/978-94-007-0372-8
700 Dixon, J.E., Bindeman, I.N., Kingsley, R.H., Simons, K.K., Le Roux, P.J., Hajewski, T.R.,
701 Swart, P., Langmuir, C.H., Ryan, J.G., Walowski, K.J., Wada, I., Wallace, P.J., 2017.
702 Light Stable Isotopic Compositions of Enriched Mantle Sources: Resolving the
703 Dehydration Paradox. Geochemistry, Geophys. Geosystems 18.

https://doi.org/10.1002/2016GC006743
Füri, E., Hilton, D.R., Halldórsson, S.A., Barry, P.H., Hahm, D., Fischer, T.P., Grönvold, K., 2010. Apparent decoupling of the He and Ne isotope systematics of the Icelandic mantle: The role of He depletion, melt mixing, degassing fractionation and air interaction. Geochim. Cosmochim. Acta 74, 3307–3332. https://doi.org/10.1016/j.gca.2010.03.023
Genske, F.S., Turner, S.P., Beier, C., Chu, M.F., Tonarini, S., Pearson, N.J., Haase, K.M., 2014. Lithium and boron isotope systematics in lavas from the Azores islands reveal crustal assimilation. Chem. Geol. 373, 27–36. https://doi.org/10.1016/j.chemgeo.2014.02.024
Gurenko, A.A., Chaussidon, M., 1997. Boron concentrations and isotopic composition of the Icelandic mantle: evidence from glass inclusions in olivine. Chem. Geol. 135, 21–34. https://doi.org/10.1016/S0009-2541(96)00102-7
Gurenko, A.A., Kamenetsky, V.S., 2011. Boron isotopic composition of olivine-hosted melt inclusions from Gorgona komatiites, Colombia: New evidence supporting wet komatiite origin. Earth Planet. Sci. Lett. 312, 201–212. https://doi.org/10.1016/j.epsl.2011.09.033
Halldórsson, S.A., Barnes, J.D., Stefánsson, A., Hilton, D.R., Hauri, E.H., Marshall, E.W., 2016a. Subducted lithosphere controls halogen enrichments in the Iceland mantle plume source. Geology 44, 679–682. https://doi.org/10.1130/G37924.1
Halldórsson, S.A., Hilton, D.R., Barry, P.H., Füri, E., Grönvold, K., 2016b. Recycling of crustal material by the Iceland mantle plume: New evidence from nitrogen elemental and isotope systematics of subglacial basalts. Geochim. Cosmochim. Acta 186, 360–364. https://doi.org/10.1016/j.gca.2016.04.051
Harðarson, B.S., Fitton, J.G., Hjartarson, Á., 2008. Tertiary volcanism in Iceland. Jökull 58, 161–178.
Hartley, M.E., de Hoog, J.C.M., Shorttle, O., 2021. Boron isotopic signatures of melt inclusions from North Iceland reveal recycled material in the Icelandic mantle source. Geochim. Cosmochim. Acta 294, 273–294. https://doi.org/10.1016/j.gca.2020.11.013
Hemond, C., Arndt, N.T., Lichtenstein, U., Hofmann, A.W., Oskarsson, N.,

735 Steinthorsson, S., 1993. The heterogeneous Iceland plume: Nd-Sr-O isotopes
736 and trace element constraints. J. Geophys. Res. 98, 15833.
737 https://doi.org/10.1029/93JB01093
738 Hervig, R.L., Moore, G.M., Williams, L.B., Peacock, S.M., Holloway, J.R., Roggensack, K.,
739 2002. Isotopic and elemental partitioning of boron between hydrous fluid and
740 silicate melt. Am. Mineral. 87, 769–774. https://doi.org/10.2138/am-2002-5-
741 620
742 Jackson, M.G., Blichert-Toft, J., Halldórsson, S.A., Mundl-Petermeier, A., Bizimis, M.,
743 Kurz, M.D., Price, A.A., Harðardóttir, S., Willhite, L.N., Breddam, K., Becker, T.W.,
744 Fischer, R.A., 2020. Ancient helium and tungsten isotopic signatures preserved
745 in mantle domains least modified by crustal recycling. Proc. Natl. Acad. Sci.
746 202009663. https://doi.org/10.1073/pnas.2009663117
747 Jakobsson, S.P., Jónasson, K., Sigurðsson, I. a., 2008. The three igneous rock series of
748 Iceland. Jökull 58, 117–138.
749 Jochum, K.P., Stoll, B., Herwig, K., Willbold, M., Hofmiann, A.W., Amini, M., Aarburg, S.,
750 Abouchami, W., Hellebrand, E., Mocek, B., Raczek, I., Stracke, A., Alard, O.,
751 Bouman, C., Becker, S., Dücking, M., Brätz, H., Klemd, R., De Bruin, D., Canil, D.,
752 Cornell, D., De Hoog, C.J., Dalpé, C., Danyushevshy, L., Eisenhauer, A., Gao, Y.,
753 Snow, J.E., Groschopf, N., Günther, D., Latkoczy, C., Guillong, M., Hauri, E.H.,
754 Höfer, H.E., Lahaye, Y., Horz, K., Jacob, D.E., Kasemann, S.A., Kent, A.J.R., Ludwig,
755 T., Zack, T., Mason, P.R.D., Meixner, A., Rosner, M., Misawa, K., Nash, B.P.,
756 Pfänder, J., Premo, W.R., Sun, W.D., Tiepolo, M., Vannucci, R., Vennemann, T.,
757 Wayne, D., Woodhead, J.D., 2006. MPI-DING reference glasses for in situ
758 microanalysis: New reference values for element concentrations and isotope
759 ratios. Geochemistry, Geophys. Geosystems 7.
760 https://doi.org/10.1029/2005GC001060
761 Kogiso, T., Tatsumi, Y., Nakano, S., 1997. Trace element transport during
762 dehydration processes in the subducted oceanic crust: 1. Experiments and
763 implications for the origin of ocean island basalts. Earth Planet. Sci. Lett. 148,
764 193–205. https://doi.org/10.1016/s0012-821x(97)00018-6
765 Kokfelt, T.F., Hoernle, K.A.J., Hauff, F., Fiebig, J., Werner, R., Garbe-scho, D., 2006.

766 Combined Trace Element and Pb-Nd-Sr-O Isotope Evidence for Recycled
767 Oceanic Crust (Upper and Lower) in the Iceland Mantle Plume. J. Petrol. 47,
768 1705–1749. https://doi.org/10.1093/petrology/egl025
769 Konrad-Schmolke, M., 2016. Slab mantle dehydrates beneath Kamchatka—Yet
770 recycles water into the deep mantle. Geochemistry Geophys. Geosystems 1000–
771 1019. https://doi.org/10.1002/2015GC006060.Received
772 Konrad-Schmolke, M., Halama, R., 2014. Combined thermodynamic-geochemical
773 modeling in metamorphic geology: Boron as tracer of fluid-rock interaction.
774 Lithos 208–209, 393–414. https://doi.org/10.1016/j.lithos.2014.09.021
775 Koornneef, J.M., Stracke, A., Bourdon, B., Meier, M.A., Jochum, K.P., Stoll, B., Grönvold,
776 K., 2012. Melting of a two-component source beneath Iceland. J. Petrol. 53, 127–
777 157. https://doi.org/10.1093/petrology/egr059
778 Maclennan, J., McKenzie, D., Grönvold, K., Shimizu, N., Eiler, J.M., Kitchen, N., 2003.
779 Melt mixing and crystallization under Theistareykir, northeast Iceland.
780 Geochemistry, Geophys. Geosystems 4.
781 https://doi.org/10.1029/2003GC000558
782 Macpherson, C.G., Hilton, D.R., Day, J.M.D., Lowry, D., Grönvold, K., 2005. High-
783 3He/4He, depleted mantle and low-δ 18O, recycled oceanic lithosphere in the
784 source of central Iceland magmatism. Earth Planet. Sci. Lett. 233, 411–427.
785 https://doi.org/10.1016/j.epsl.2005.02.037
786 Magna, T., Wiechert, U., Stuart, F.M., Halliday, A.N., Harrison, D., 2011. Combined Li-
787 He isotopes in Iceland and Jan Mayen basalts and constraints on the nature of
788 the North Atlantic mantle. Geochim. Cosmochim. Acta 75, 922–936.
789 https://doi.org/10.1016/j.gca.2010.11.007
790 Marschall, H.R., 2018. Boron Isotopes in the Ocean Floor Realm and the Mantle, in:
791 Boron Isotopes, Advances in Isotope Geochemistry. pp. 189–215.
792 https://doi.org/10.1007/978-3-319-64666-4_8
793 Marschall, H.R., Altherr, R., Rüpke, L., 2007. Squeezing out the slab - modelling the
794 release of Li, Be and B during progressive high-pressure metamorphism. Chem.
795 Geol. 239, 323–335. https://doi.org/10.1016/j.chemgeo.2006.08.008
796 Marschall, H.R., Monteleone, B.D., 2015. Boron Isotope Analysis of Silicate Glass with

797 Very Low Boron Concentrations by Secondary Ion Mass Spectrometry.
798 Geostand. Geoanalytical Res. 39, 31–46. https://doi.org/10.1111/j.1751-
799 908X.2014.00289.x
800 Marschall, H.R., Wanless, V.D., Shimizu, N., Pogge von Strandmann, P.A.E., Elliott, T.,
801 Monteleone, B.D., 2017. The boron and lithium isotopic composition of mid-
802 ocean ridge basalts and the mantle, Geochimica et Cosmochimica Acta. Elsevier
803 Ltd. https://doi.org/10.1016/j.gca.2017.03.028
804 Michael, P.J., Cornell, W.C., 1998. Influence of spreading rate and magma supply on
805 crystallization and assimilation beneath mid-ocean ridges: Evidence from
806 chlorine and major element chemistry of mid-ocean ridge basalts. J. Geophys.
807 Res. Solid Earth 103, 18325–18356. https://doi.org/10.1029/98jb00791
808 Óskarsson, N., Sigvaldason, G.E., Steinthórsson, S., 1982. A dynamic model of rift
809 zone petrogenesis and the regional petrology of Iceland. J. Petrol. 23, 28–74.
810 https://doi.org/10.1093/petrology/23.1.28
811 Palmer, M.R., Sturchio, N.C., 1990. The boron isotope systematics of the Yellowstone
812 National Park (Wyoming) hydrothermal system: A reconnaissance. Geochim.
813 Cosmochim. Acta 54, 2811–2815. https://doi.org/10.1016/0016-
814 7037(90)90015-D
815 Peate, D.W., Breddam, K., Baker, J.A., Kurz, M.D., Barker, A.K., Prestvik, T., Grassineau,
816 N., Skovgaard, A.C., 2010. Compositional characteristics and spatial distribution
817 of enriched Icelandic mantle components. J. Petrol. 51, 1447–1475.
818 https://doi.org/10.1093/petrology/egq025
819 Raffone, N., Ottolini, L.P., Tonarini, S., Gianelli, G., D'Orazio, M., Fridleifsson, G.Ó.,
820 2010. An investigation of trace and isotope light elements in mineral phases
821 from well RN-17 (Reykjanes Peninsula, SW Iceland). IOP Conf. Ser. Mater. Sci.
822 Eng. 7, 012026. https://doi.org/10.1088/1757-899X/7/1/012026
823 Rasmussen, M.B., Halldórsson, S.A., Gibson, S.A., Guðfinnsson, G.H., 2020. Olivine
824 chemistry reveals compositional source heterogeneities within a tilted mantle
825 plume beneath Iceland. Earth Planet. Sci. Lett. 531, 116008.
826 https://doi.org/10.1016/j.epsl.2019.116008
827 Rose-Koga, E.F., Sigmarsson, O., 2008. B-O-Th isotope systematics in Icelandic

828 tephra. Chem. Geol. 255, 454–462.
829 https://doi.org/10.1016/j.chemgeo.2008.07.013
830 Rudge, J.F., Maclennan, J., Stracke, A., 2013. The geochemical consequences of mixing
831 melts from a heterogeneous mantle. Geochim. Cosmochim. Acta 114, 112–143.
832 https://doi.org/10.1016/j.gca.2013.03.042
833 Ryan, J.G., Leeman, W.P., Morris, J.D., Langmuir, C.H., 1996. The boron systematics of
834 intraplate lavas: Implications for crust and mantle evolution. Geochim.
835 Cosmochim. Acta 60, 415–422. https://doi.org/10.1016/0016-
836 7037(95)00402-5
837 Shorttle, O., Maclennan, J., 2011. Compositional trends of Icelandic basalts:
838 Implications for short-length scale lithological heterogeneity in mantle plumes.
839 Geochemistry, Geophys. Geosystems 12.
840 https://doi.org/10.1029/2011GC003748
841 Smith, H.J., Spivack, A.J., Staudigel, H., Hart, S.R., 1995. The boron isotopic
842 composition of altered oceanic crust. Chem. Geol. 126, 119–135.
843 https://doi.org/10.1016/0009-2541(95)00113-6
844 Stracke, A., Bizimis, M., Salters, V.J.M., 2003a. Recycling oceanic crust: Quantitative
845 constraints. Geochemistry, Geophys. Geosystems 4.
846 https://doi.org/10.1029/2001GC000223
847 Stracke, A., Zindler, A., Salters, V.J.M., McKenzie, D., Blichert-Toft, J., Albarède, F.,
848 Grönvold, K., 2003b. Theistareykir revisited. Geochemistry, Geophys.
849 Geosystems 4. https://doi.org/10.1029/2001GC000201
850 Tanaka, R., Nakamura, E., 2005. Boron isotopic constraints on the source of
851 Hawaiian shield lavas. Geochim. Cosmochim. Acta 69, 3385–3399.
852 https://doi.org/10.1016/j.gca.2005.03.009
853 Thirlwall, M.F., Gee, M.A.M., Lowry, D., Mattey, D.P., Murton, B.J., Taylor, R.N., 2006.
854 Low δ 18 O in the Icelandic mantle and its origins: Evidence from Reykjanes
855 Ridge and Icelandic lavas. Geochim. Cosmochim. Acta 70, 993–1019.
856 https://doi.org/10.1016/j.gca.2005.09.008
857 Thirlwall, M.F., Gee, M.A.M., Taylor, R.N., Murton, B.J., 2004. Mantle components in
858 Iceland and adjacent ridges investigated using double-spike Pb isotope ratios.

859 Geochim. Cosmochim. Acta 68, 361–386. https://doi.org/10.1016/S0016-
860 7037(03)00424-1
861 Wada, I., Behn, M.D., Shaw, A.M., 2012. Effects of heterogeneous hydration in the
862 incoming plate, slab rehydration, and mantle wedge hydration on slab-derived
863 H2O flux in subduction zones. Earth Planet. Sci. Lett. 353–354, 60–71.
864 https://doi.org/10.1016/j.epsl.2012.07.025
865 Walowski, K.J., Kirstein, L.A., De Hoog, J.C.M., Elliott, T., Savov, I.P., Jones, R.E., EIMF,
866 2021. Boron recycling in the mantle: Evidence from a global comparison of
867 ocean island basalts. Geochim. Cosmochim. Acta 302, 83–100.
868 https://doi.org/10.1016/j.gca.2021.03.017
869 Walowski, K.J., Kirstein, L.A., De Hoog, J.C.M., Elliott, T.R., Savov, I.P., Jones, R.E., 2019.
870 Investigating ocean island mantle source heterogeneity with boron isotopes in
871 melt inclusions. Earth Planet. Sci. Lett. 508, 97–108.
872 https://doi.org/10.1016/j.epsl.2018.12.005
873 Walowski, K.J., Wallace, P.J., Hauri, E.H., Wada, I., Clynne, M.A., 2015. Slab melting
874 beneath the Cascade Arc driven by dehydration of altered oceanic peridotite.
875 Nat. Geosci. 8, 404–408. https://doi.org/10.1038/ngeo2417
876 Wang, X.J., Chen, L.H., Hofmann, A.W., Hanyu, T., Kawabata, H., Zhong, Y., Xie, L.W.,
877 Shi, J.H., Miyazaki, T., Hirahara, Y., Takahashi, T., Senda, R., Chang, Q., Vaglarov,
878 B.S., Kimura, J.I., 2018. Recycled ancient ghost carbonate in the Pitcairn mantle
879 plume. Proc. Natl. Acad. Sci. U. S. A. 115, 8682–8687.
880 https://doi.org/10.1073/pnas.1719570115
881 White, W.M., 2015. Isotopes, DUPAL, LLSVPs, and Anekantavada. Chem. Geol. 419,
882 10–28. https://doi.org/10.1016/j.chemgeo.2015.09.026
883 Workman, R.K., Hart, S.R., Jackson, M., Regelous, M., Farley, K.A., Blusztajn, J., Kurz,
884 M., Staudigel, H., 2004. Recycled metasomatized lithosphere as the origin of the
885 Enriched Mantle II (EM2) end-member: Evidence from the Samoan Volcanic
886 Chain. Geochemistry, Geophys. Geosystems 5, 1–44.
887 https://doi.org/10.1029/2003GC000623
888 Yamaoka, K., Ishikawa, T., Matsubaya, O., Ishiyama, D., Nagaishi, K., Hiroyasu, Y.,
889 Chiba, H., Kawahata, H., 2012. Boron and oxygen isotope systematics for a

complete section of oceanic crustal rocks in the Oman ophiolite. Geochim. Cosmochim. Acta 84, 543–559. https://doi.org/10.1016/j.gca.2012.01.043

Zindler, A., Hart, S., 1986. Chemical Geodynamics. Annu. Rev. Earth Planet. Sci. 14, 493–571. https://doi.org/10.1146/annurev.ea.14.050186.002425

FIGURES

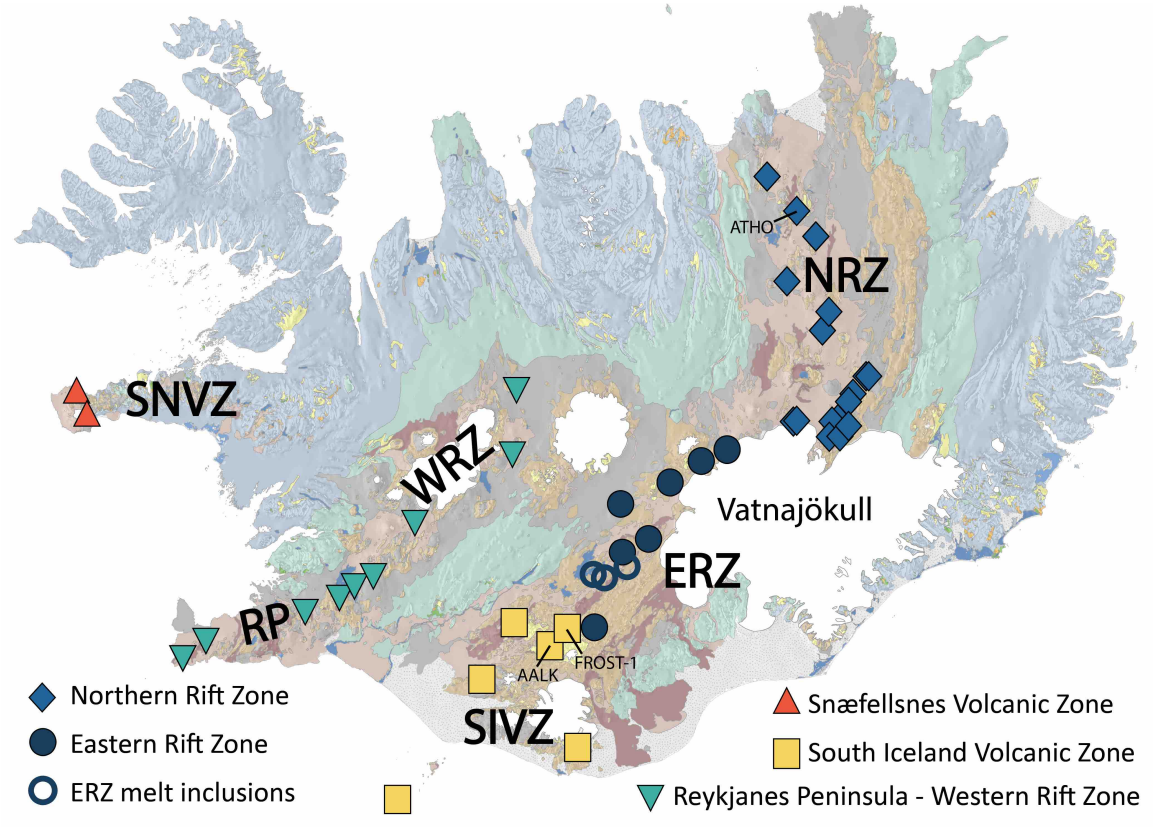

Figure 1: Locality map of sample locations. Symbols on the map match symbols used in the figures. The coloration of the base map is a geologic map of Iceland, where light blue along the outer parts of Iceland represent Tertiary lavas, the dark pink in the interior represents lavas erupted since the end of the Pleistocene. Rhyolites (A-ALK and A-THO) and icelandites (FROST-1) are labelled for reference.

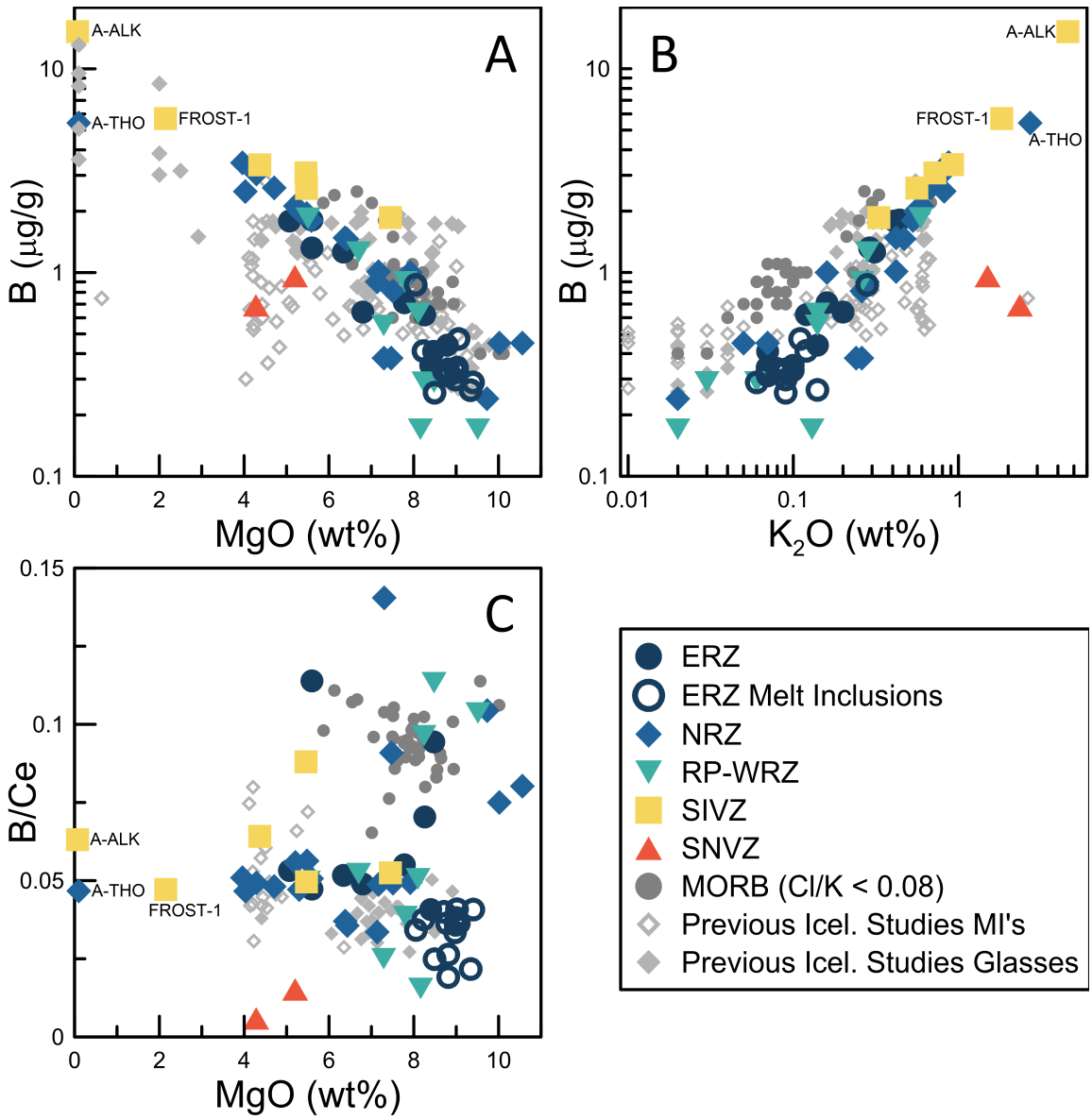

Figure 2: MgO versus boron concentration (A), K_2O versus boron concentration (B), and MgO versus B/Ce (C). Rhyolites (A-ALK and A-THO) and icelandites (FROST-1) are labelled for reference. References for basalts from previous Iceland studies are in Figure 3.

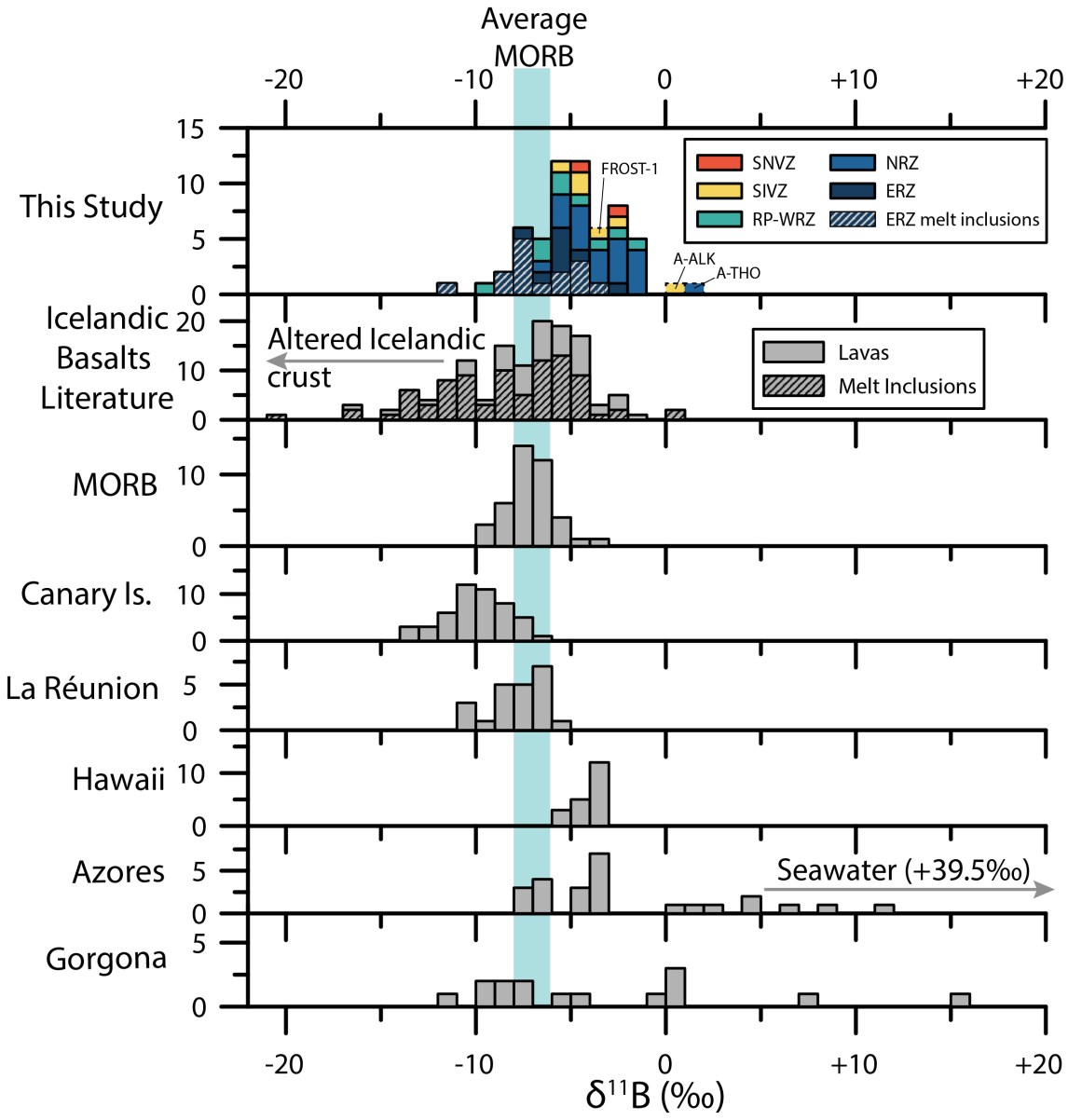

Figure 3: Histograms of the boron isotope compositions of basaltic OIB lavas, melt inclusions, and MORBs. Rhyolites (A-ALK and A-THO) and icelandites (FROST-1) are labelled for reference. Data from previous Icelandic studies are from Gurenko & Chaussidon (1997), Rose-Koga & Sigmarsson (2008), Brounce et al. (2012), and Hartley et al. (2020). MORB represents MORB lavas with Cl/K < 0.08 from Marschall et al. (2017). Canary Islands and Reunion data come from Walowski et al. (2019). Hawaii data come from Tanaka and Nakamura (2005). Azores data are from Genske et al. (2014). Gorgona data come from Gurenko and Kamenetsky (2011).

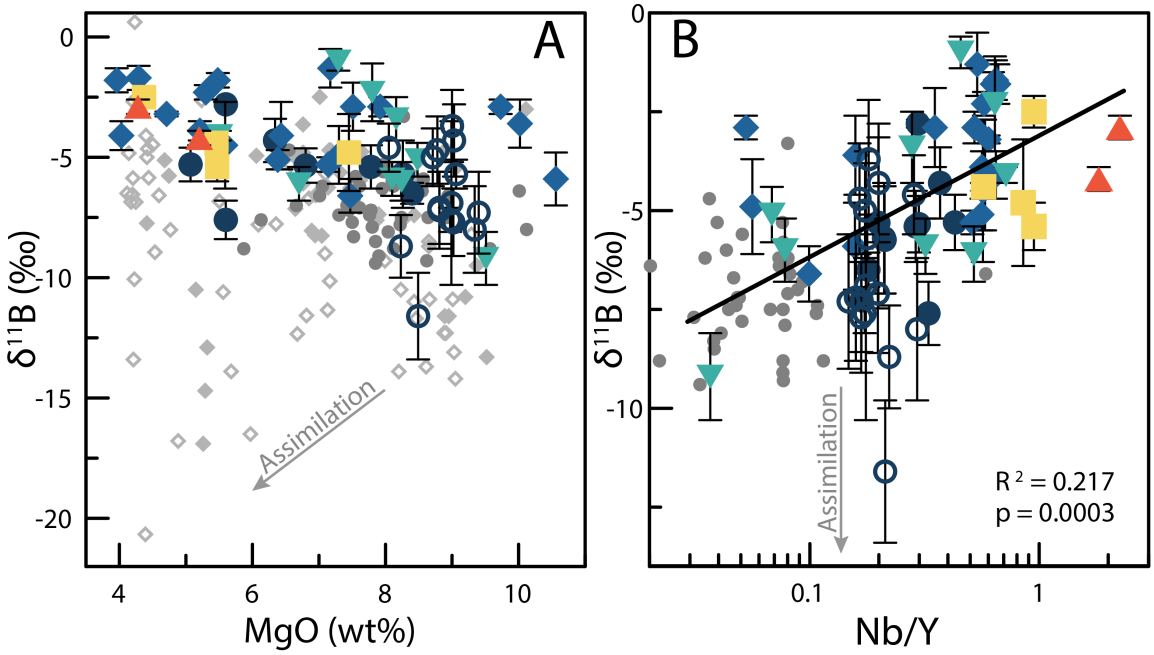

Figure 4: MgO versus $\delta^{11}B$ (A) and Nb/Y vs $\delta^{11}B$ (B) in Icelandic basaltic lavas and melt inclusions. In (B), R^2 is the correlation coefficient and the *p* value measures its statistical significance, the MORB data is not included in the regression. For more plots of correlations between $\delta^{11}B$ and trace element ratio indicators of source heterogeneity, see Figure S4. The arrows labelled "assimilation" indicate the approximaate direction of geochemical change generated by assimilation. Symbols as in Figure 2.

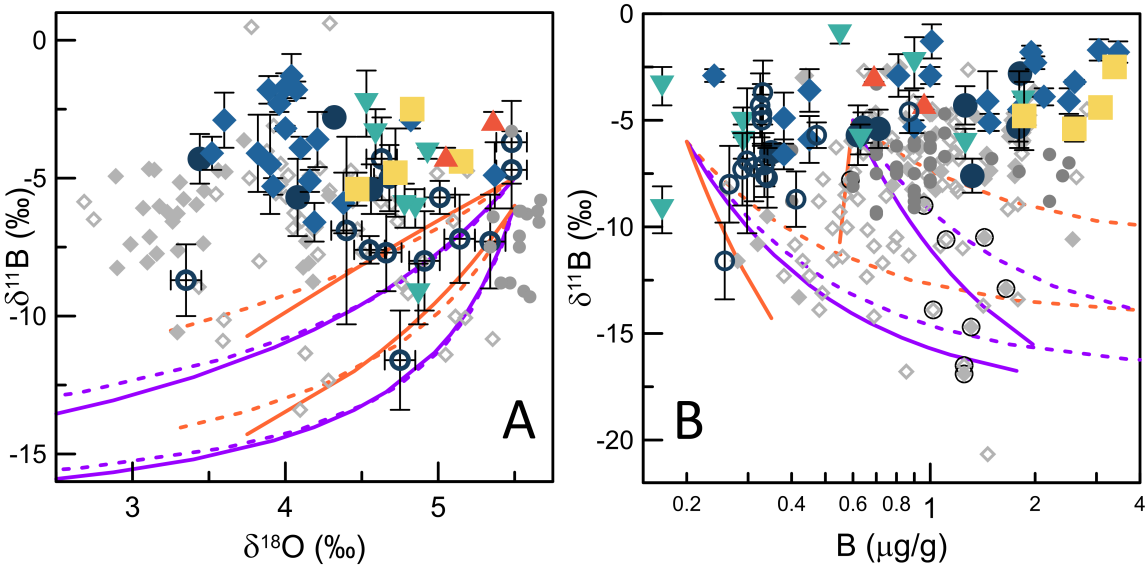

Figure 5: $\delta^{18}O$ versus $\delta^{11}B$ (A) and B versus $\delta^{11}B$ (B) in Icelandic basalt lavas and melt inclusions. Symbols are the same as in Figure 2. The circled literature analyses in (B) indicate the samples of Brounce et al. (2012) from Lakigígar that were previously interpreted to have sustained high degrees of crustal assimilation. The solid and dashed lines in both figures are mixing and assimilation-fractional crystallization (AFC) models, respectively. Two sets of mixing and AFC models are calculated to simulate assimilation into a more primitive melt and a more evolved melt. The composition of the assimilation endmembers is presented in the supplementary information; orange curves represent a "low-T altered bulk upper crust" type assimilant ([B] = 0.5 μg/g, $\delta^{11}B$ = -17.6‰, $\delta^{18}O$ = +2‰), blue lines represent a "high-T hydrothermally altered basalt" composition ([B] = 3.34 μg/g, $\delta^{11}B$ = -17.4‰, $\delta^{18}O$ = -5‰). Mixing models curves end at 50% mixing, AFC model curves end at 90% crystallization and are calculated using a M_a/M_c of 0.5. Error bars represent 1SD.

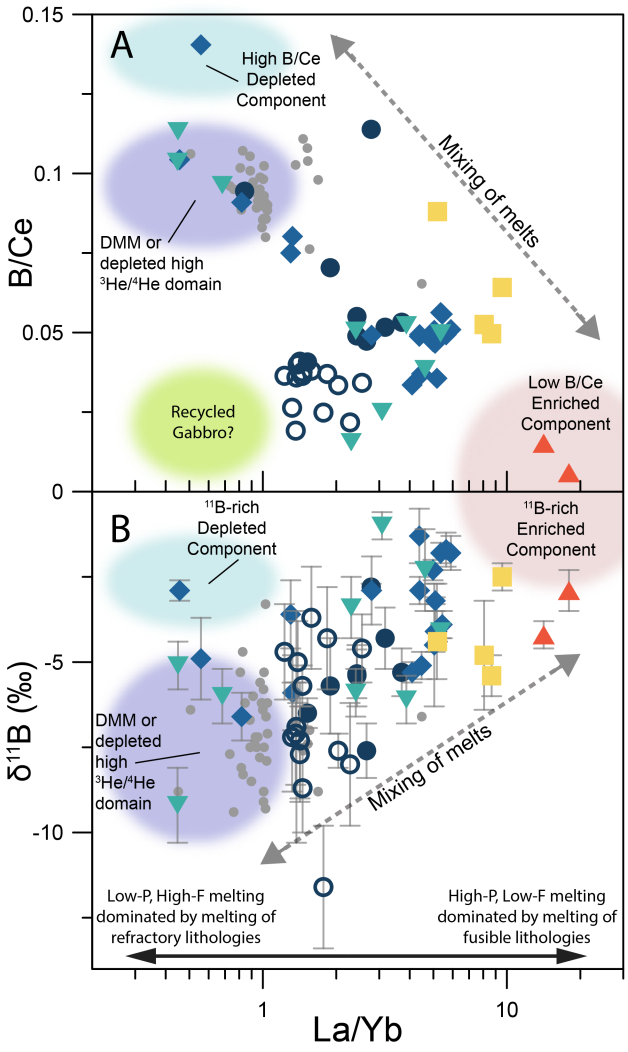

Figure 6: La/Yb versus B/Ce (A) and $\delta^{11}B$ (B). The symbols follow those in Figure 2. The colored regions represent the approximate composition of potential components within the Icelandic mantle source, as suggested by B/Ce and $\delta^{11}B$ systematics. The dark blue region on the left represents basalt melts that have MORB-like B/Ce and $\delta^{11}B$ values, which could be generated either by DMM or ancient high $^{3}He/^{4}He$ domains. The blue-green region just above the dark blue region represents a refractory and depleted high B/Ce and high $\delta^{11}B$ value component. The light orange region on the right represents a fertile and enriched component with high $\delta^{11}B$ values and low B/Ce ratios. The lime-green region in (A) represents the composition of depleted recycled gabbro cumulates. The spectrum of melts observed in Iceland can be explained by melt mixing and aggregation between these components (dashed line is schematic, not a model). See section 6.2 for details.

959

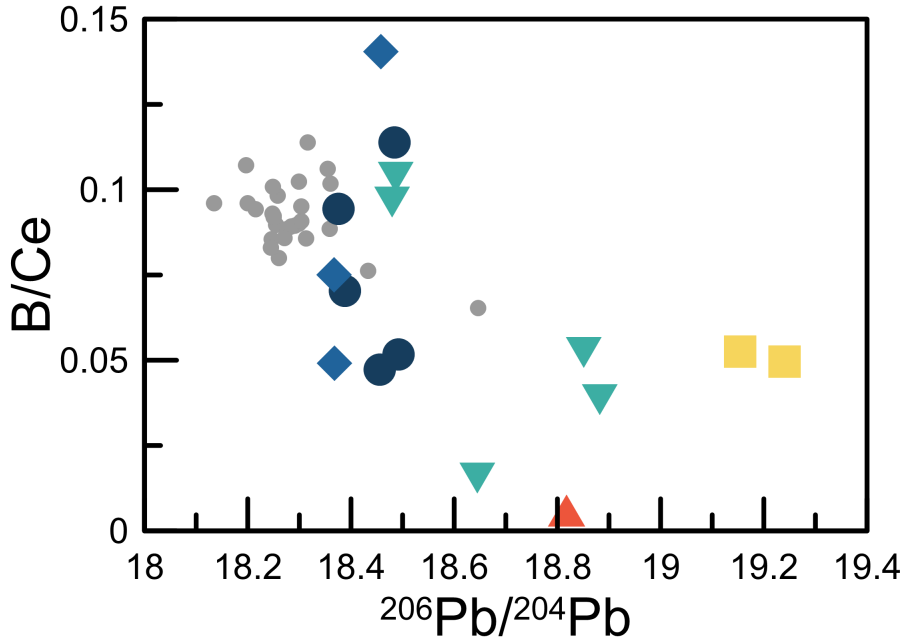

960

961 Figure 7: $^{206}Pb/^{204}Pb$ versus B/Ce in Icelandic glasses and MORB. Note that all

962 samples with $^{206}Pb/^{204}Pb$ greater than 18.6 have lower B/Ce than samples with

963 $^{206}Pb/^{204}Pb$ less than 18.6. Symbols as in Figure 2.

964

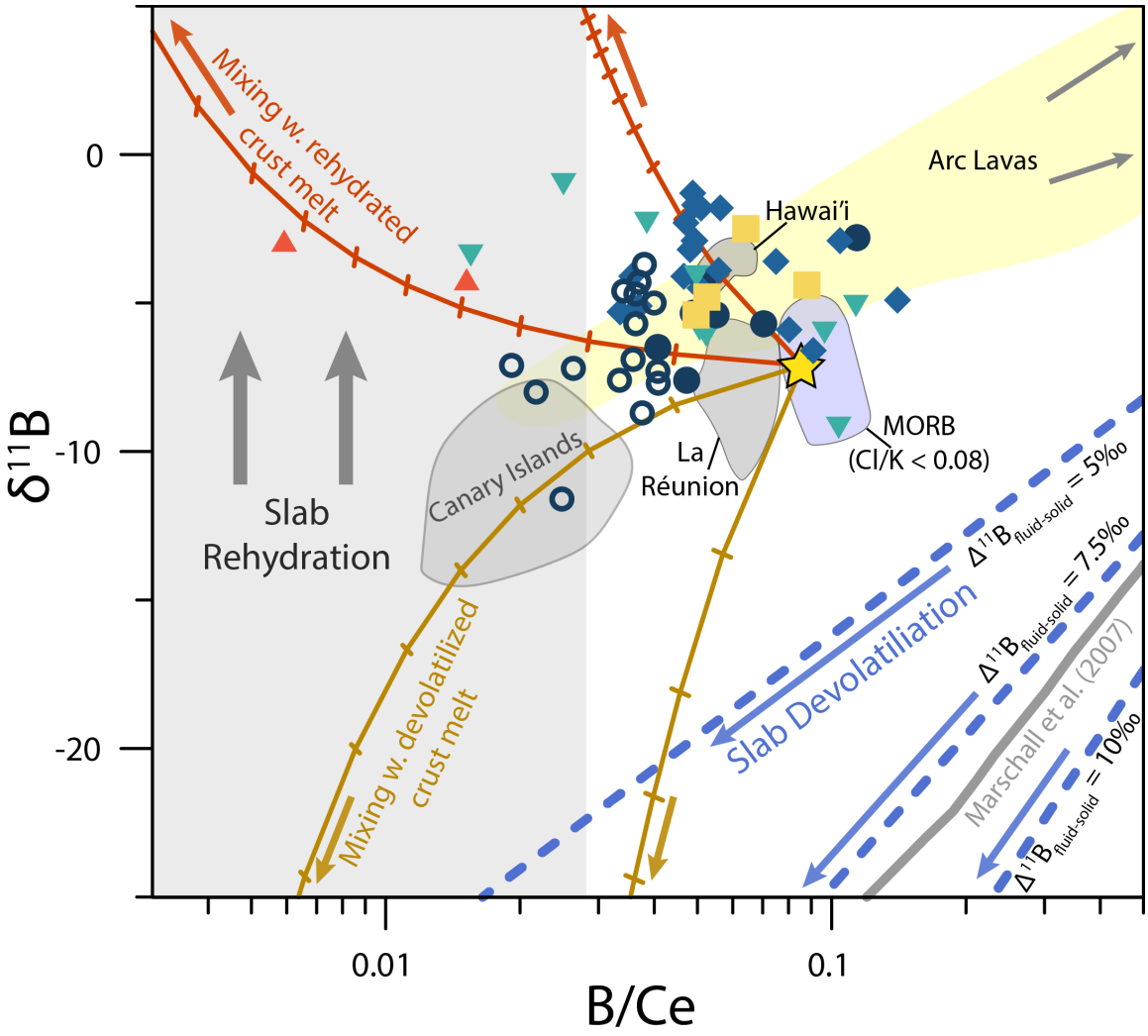

Figure 8: B/Ce versus $\delta^{11}B$ values in basalts and melt inclusions from Iceland. Other OIB localities and MORB are represented by the gray and light blue fields, respectively. The yellow star in the center represents the composition of average MORB. The yellow field represents the distribution of arc lavas from De Hoog & Savov (2017). The four lines radiating towards the left from the star represent mixing lines between MORB and aggregate melts generated from 6% fractional melting of rehydrated subducted ocean crust (upper red lines) and devolatilized subducted ocean crust (lower orange lines). The tick marks represent units of 10% mixing. The devolatilized endmembers used in this model have compositions: B/Ce = 0.03 and $\delta^{11}B$ = -33.42‰ (right curve); B/Ce = 0.003 and $\delta^{11}B$ = -50.0‰ (left curve). The rehydrated endmembers used in this model have compositions: B/Ce = 0.03 and $\delta^{11}B$ = +5‰ (right curve); B/Ce = 0.003 and $\delta^{11}B$ = +5‰ (left curve). The

three dashed blue lines and thick grey line represent the devolatilization paths of subducting oceanic crust, calculated using simple Rayleigh fractionation models and the thermo-chemical model of Marschall et al. (2007) respectively. Although calculated using a different approach, the model of Marschall et al. approximately corresponds to a Rayleigh fractionation model with $\Delta^{11}B_{fluid\text{-}solid}$ = +8‰. The grey field on the left marks the range of possible rehydrated crust compositions. See section 6.4 for additional details.